Simulation of the Present and Future Climate Change with the GISS ModelE2

Larissa Nazarenko, Nick Tausnev, Gavin Schmidt,
Ron Miller, Max Kelley, Reto Ruedy

NASA Goddard Institute for Space Studies

GISS Climate Model, modelE2

- We use new version of NASA Goddard Institute for Space Studies (GISS) climate model, modelE2 with 2º by 2.5º horizontal resolution and 40 vertical layers in atmosphere, with the model top at 0.1 hPa:

  ◦ NINT - non-interactive version of atmospheric model with three-dimensional distributions of ozone and aerosols specified as decadal concentrations from off-line calculations [*Koch et al.,* 2011; *Shindell et al, 2009*]; with tuned aerosol indirect effect based on an empirical relation between aerosol number concentrations and clouds and adjusted to produce -1 W/m^2 TOA radiative imbalance in 2000 relative to 1850 [*Hansen et al.,* 2005].

  ◦ TCAD - fully interactive aerosols and chemistry both in the troposphere and stratosphere. All chemical species are simulated prognostically consistent with atmospheric physics in the model [*Shindell et al*., 2006]. The indirect effect of aerosols is tuned in the same way as in the NINT climate model.

  ◦ TCADI includes a parameterization of the first indirect aerosol effect on clouds following *Menon et al.* [2010]. Increased aerosol concentration leads to the decreaseof cloud droplet size, which makes clouds brighter and more reflective [*Twomey*, 1977].

Ocean Models

- E2-R – the Russell ocean model with horizontal resolution 1.25° longitude by 1° latitude, and 32 vertical levels:
  a. C-grid for the momentum equations;
  b. KPP parameterization for vertical mixing [*Large et al.,* 1994];
  c. Gent-McWilliams parameterization for the mixing effect associated with mesoscale eddies [*Gent and McWilliams,* 1990];
  d. no flux corrections.

- E2-H – the HYCOM [*Bleck*, 2006; *Sun and Bleck,* 2006], the hybrid coordinate version of the Miami Isopycnal Coordinate Ocean Model:
  a. The horizontal resolution is 1°×1°cos(latitude), 1° × 1/3° is at the equator, 26 vertical levels;
  b. an isopycnal coordinate - in the oceanic interior; z coordinate – near surface;
  c. the Kraus-Turner type vertical mixing;
  d. 2nd order flux-corrected transports.

- The sea ice model with dynamics and thermodynamics of ice cover in the Arctic and Antarctic based on the Hibler viscous-plastic rheology [*Zhang and Rothrock*, 2000] and four-layer thermodynamic ice model [*Russell et al.*, 2000].

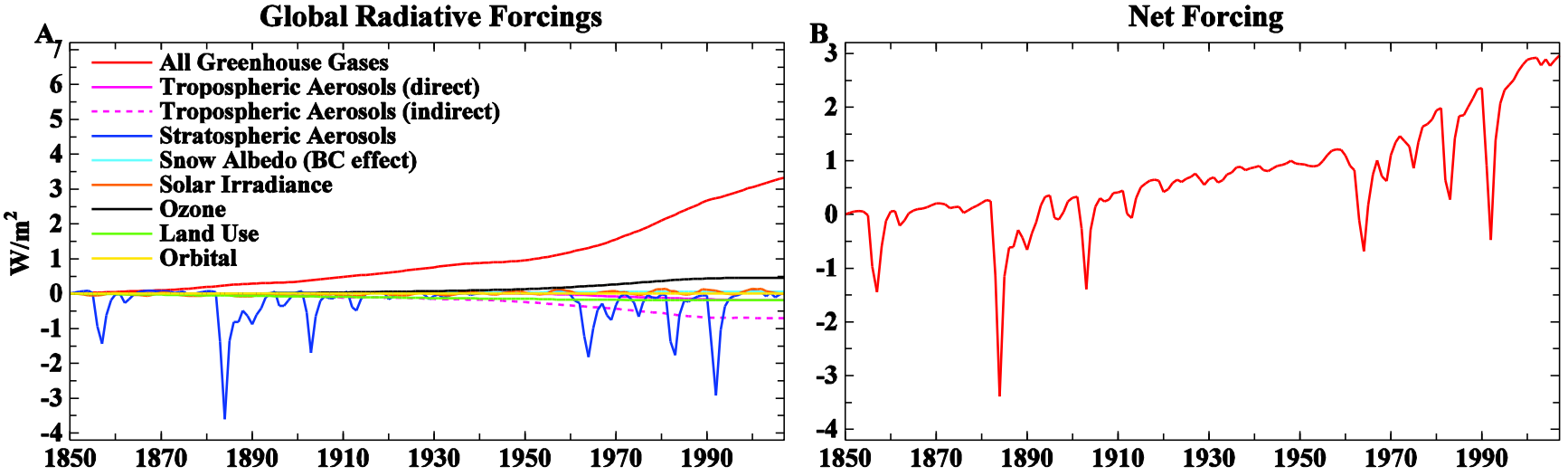

The anthropogenic forcings: time-varying well-mixed greenhouse gases, ozone (O_3), tropospheric aerosols (sulfates, nitrates, black carbon and organic carbon), stratospheric water vapor from methane oxidation, a parameterized indirect effect of aerosols on clouds, soot effect on snow and ice albedos, and land use changes.

The natural forcings : volcanic aerosols, solar irradiance, and Earth orbital parameters.

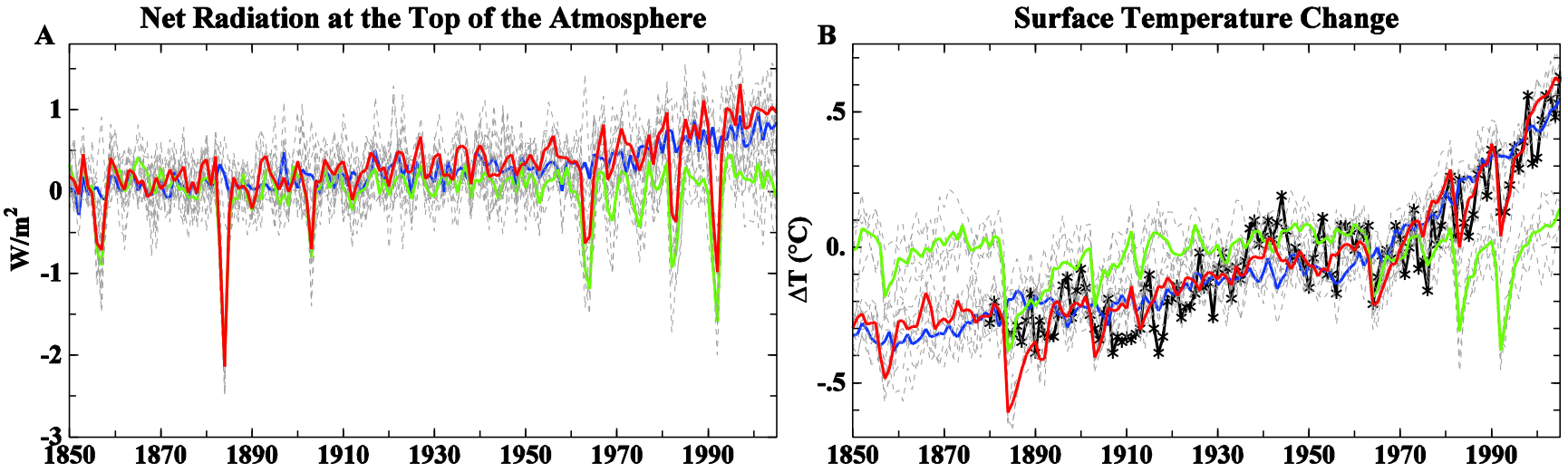

(A) Net radiation at the top of the atmosphere in the climate simulations.
ALL – imbalance 0.7 W/m2, warming +0.72°C (red lines);
ANT – stronger imbalance 0.8 W/m2 (blue lines);
NAT - imbalance -0.05 W/m2 (green lines).

(B) Simulated and observed temperature anomalies relative to the time period 1951-1980.

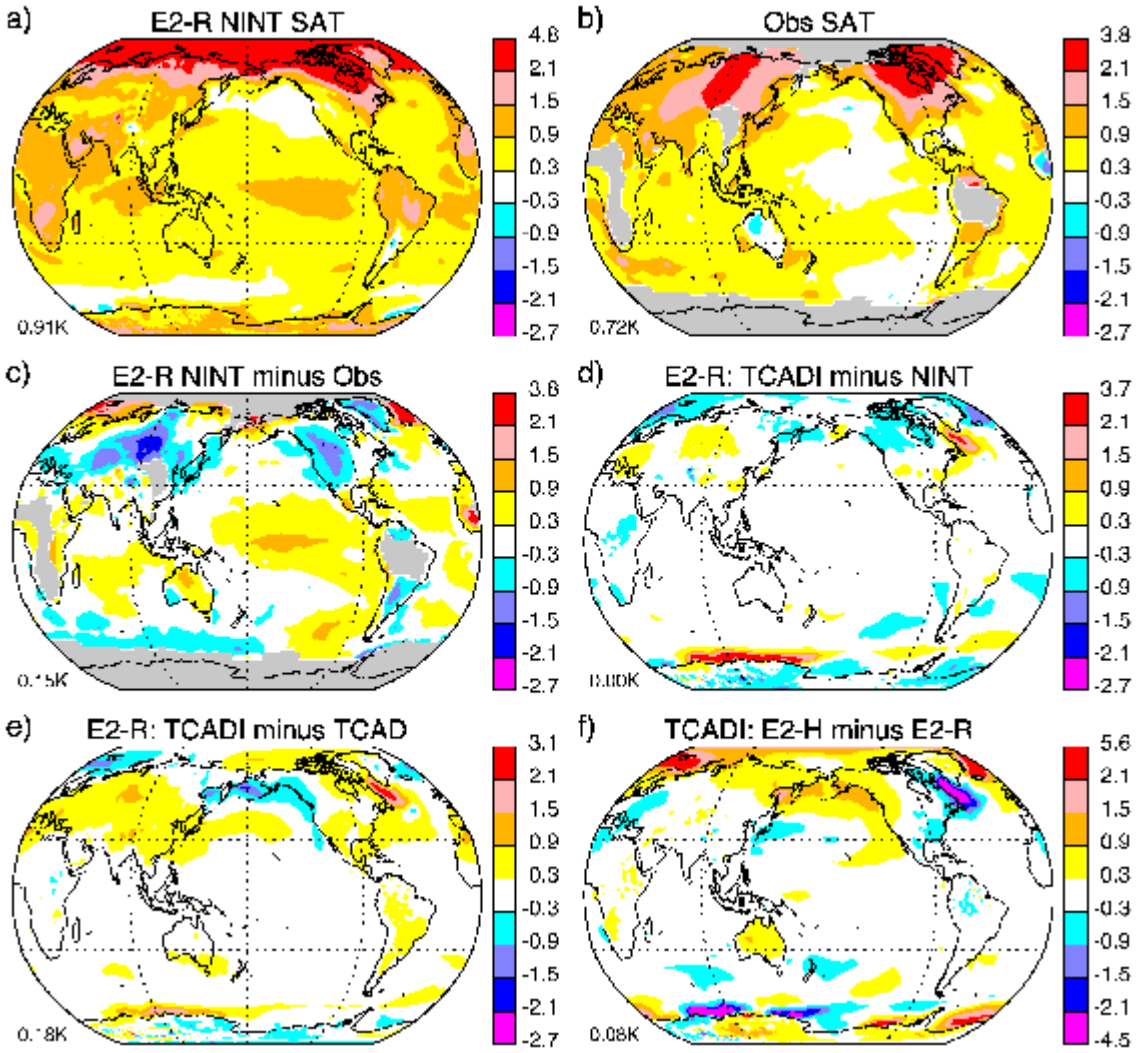

Surface air temperature difference of the decadal means: 1996-2005 and 1880-1889.

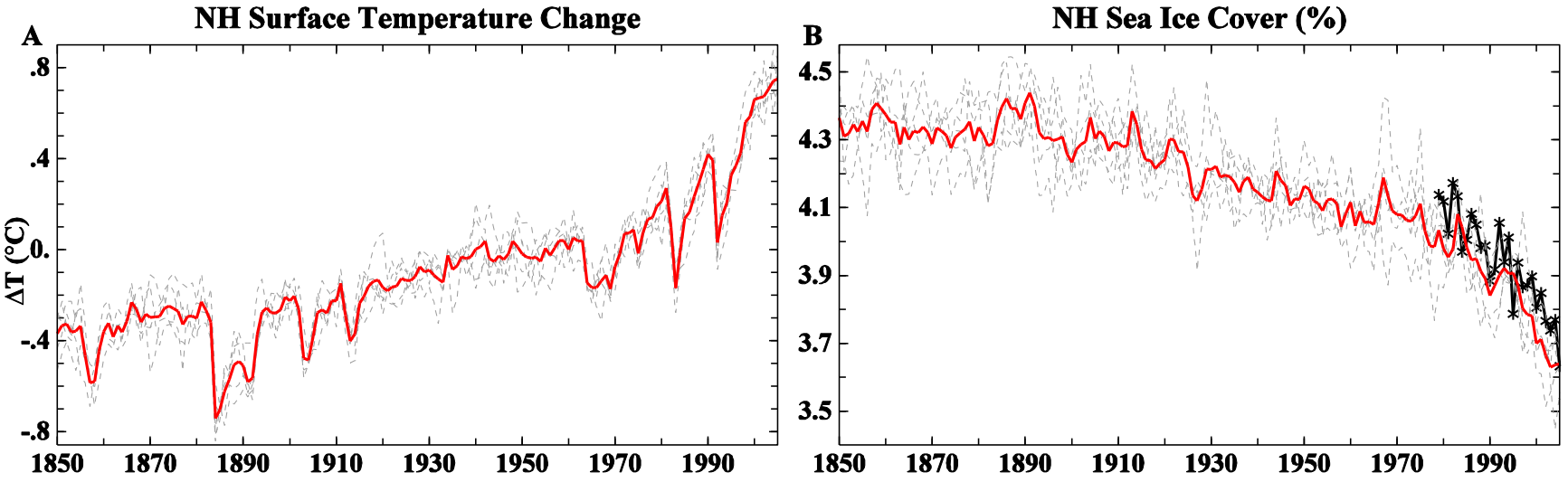

A) Simulated Northern Hemisphere surface air temperature anomalies relative to the base period 1951-1980.
Arctic amplification – warming +0.8°C (based on linear trend).

(B) Simulated and observed Northern Hemisphere sea ice cover in per cent of the Northern Hemisphere area.
The Northern Hemisphere NSIDC sea ice cover - 9.8% decrease from 1979 to 2005; simulated Arctic Ocean ice area decrease – 10.2%.

Strong negative correlation of -0.8 between the Northern Hemisphere surface air temperature and sea ice area.

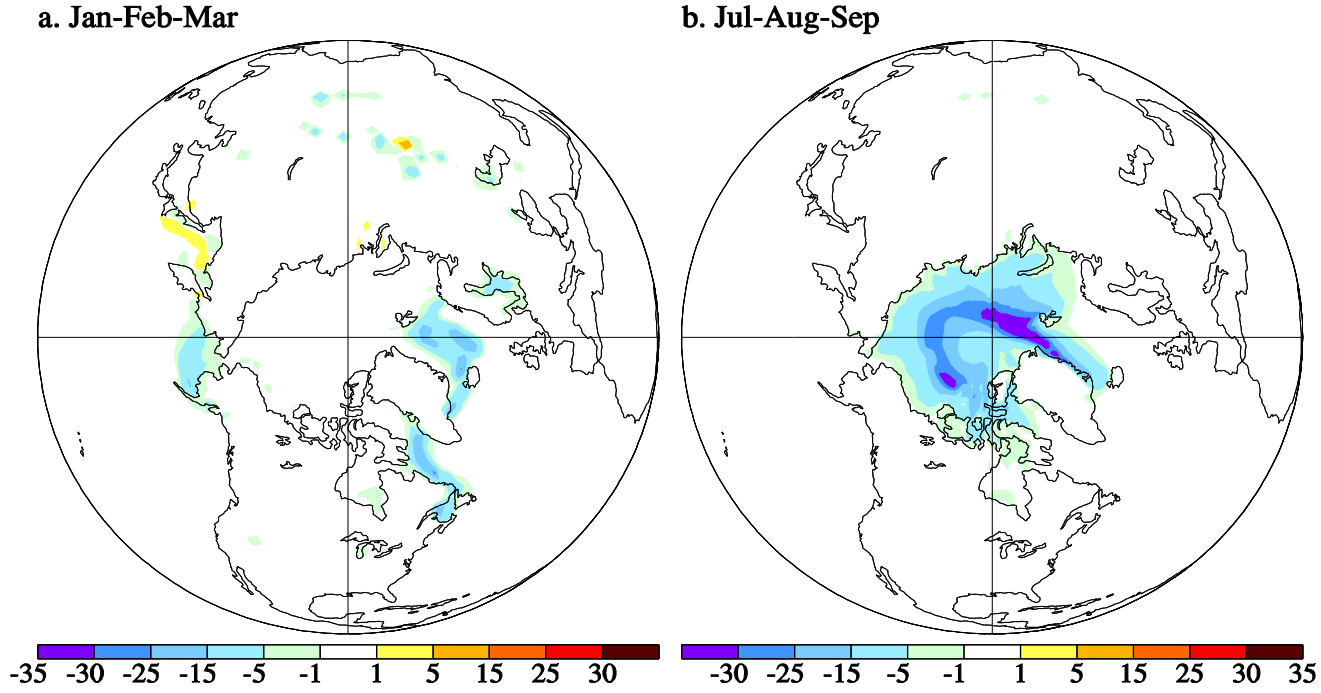

(A) Changes in winter (January-February-March) Northern Hemisphere ice cover between 1996-2005 and 1961-1970 - 3.1% ;

(B) for summer (July-August-September) - 31.8% .

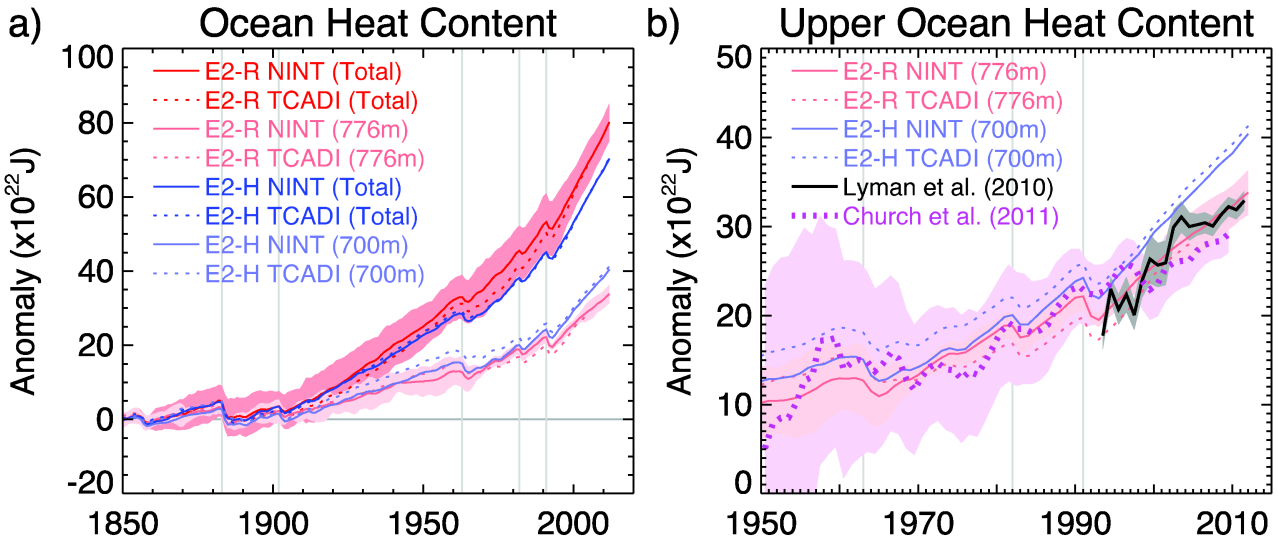

a) Ocean Heat Content Anomalies :

- The heat content of the GISS-E2-H ensembles is lower, indicating that ocean heat uptake is significantly smaller.
- The GISS-E2-H ensemble accumulates more heat in the upper ocean compared to the corresponding GISS-E2-R model.
- The GISS-E2-R ensembles transfer heat into the deep ocean to a greater extent, slowing the warming at the surface.

b) Upper Ocean Heat Content Anomalies :

- The warming in the GISS-E2-R ensembles is in agreement with the trend inferred by both observational analyses.
- The GISS-E2-H ensembles warm excessively, partly because of insufficient heat export to the deep ocean below 700 m.

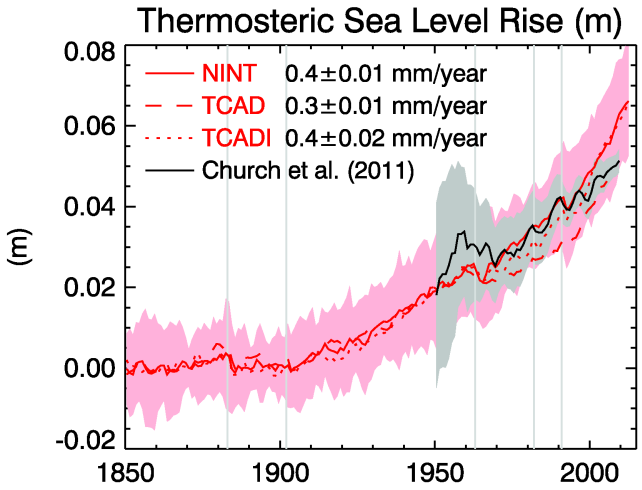

The thermosteric component of sea level rise is calculated from the density change corresponding to changes in temperature and salinity.

- Between 1900 and 1990, the trend of each ensemble is one third of the trend during the past two decades.
- Between 1993 and 2009, the modeled thermosteric contribution to sea level increases by just over 1mm per year in each ensemble: twice the observed trend of 0.65±0.12 mm per year.
- Since the pre-industrial, the total sea level rise is estimated near 210 mm (Church and White, 2011). The thermosteric change of the NINT and TCAD ensembles is 65 ± 15 mm, about one-third of the total observed value.

	GISS-E2-R			GISS-E2-H			GISS-ER	
	NINT	TCAD	TCADI	NINT	TCAD	TCADI	(NINT)	Obs.
N. Atl. MOC (Max)	27.2±0.7	26.6±0.5	24.5±2.6	24.5± 0.8	25.2± 0.5	22.7± 0.6	26±1	-
N. Atl. MOC (26°N)	18.4±0.3	18.0±0.4	17.2±1	22.4±0.6	23.1±0.3	20.4±0.5	19±0.5	$\approx 17^{R11}$
Atl. Heat 26°N	0.97±0.01	0.96±0.02	0.92±0.07	0.99±0.02	1.02±0.01	0.99±0.02	0.86	1.3 ± 0.4^{J11}
ACC transport (Drakes Pass.)	254± 1	251± 1	254± 1	192±2	192±1	190±1	225	$\approx 130^{P88}$
Gulf Stream	49± 1	47±2	45±2	39.8±0.8	39.2±0.8	41.0±0.5	33±1	$\approx 35^{R11}$
Kuroshio	64±1	67±2	64±1	71.7±0.5	72.1±0.5	74.5±1.4	43±1	$\approx 57^{I01}$
Bering Str.	0.16±0.01	0.16±0.01	0.16±0.01	0.45±0.01	0.46±0.01	0.46±0.01	0.05±0.04	0.8 ± 0.2^{W05}
Indonesian throughflow	11.5±0.2	11.4±0.2	11.7±0.6	17.6±0.3	18.5±0.5	17.5±0.5	6.2±0.6	15^{S09}

Selected ocean mass (Sv) and heat (PW) fluxes. Range is standard deviation of the 1980-2004 average from 5 ensemble members for each configuration. Observations: R11 – Rainer et al. (2011); P88 – Petersen (1988); J11 – Johns et al. (2011); I01 – Imawaki et al. (2001); W05 – Woodgate et al. (2005); S09 – Sprintall et al. (2009).

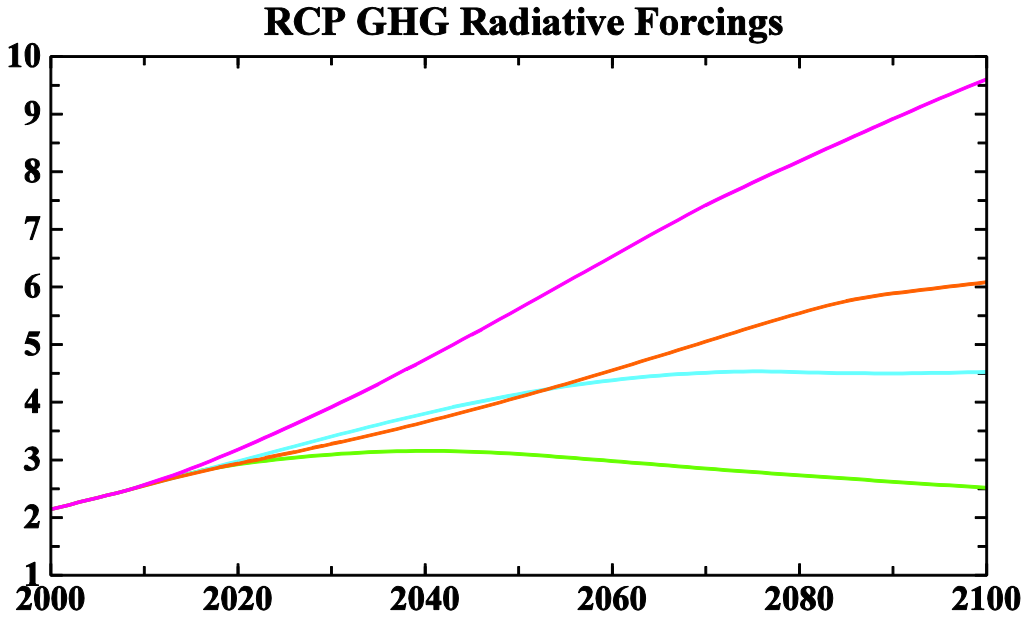

Instantaneous global GHG climate forcings used in global future climate simulations relative to their values in 1950.

RCP2.6 (green line) – the lowest forcing scenario (RCP3PD – Peak Decline from around 2050 to 2100)
RCP4.5 (blue line) – a stabilization scenario, radiative forcings are kept stable during the last three decades
RCP6.0 (orange line) - a medium baseline or a high mitigation scenario.
RCP8.5 (pink line) – the most dramatic business-as-usual scenario.

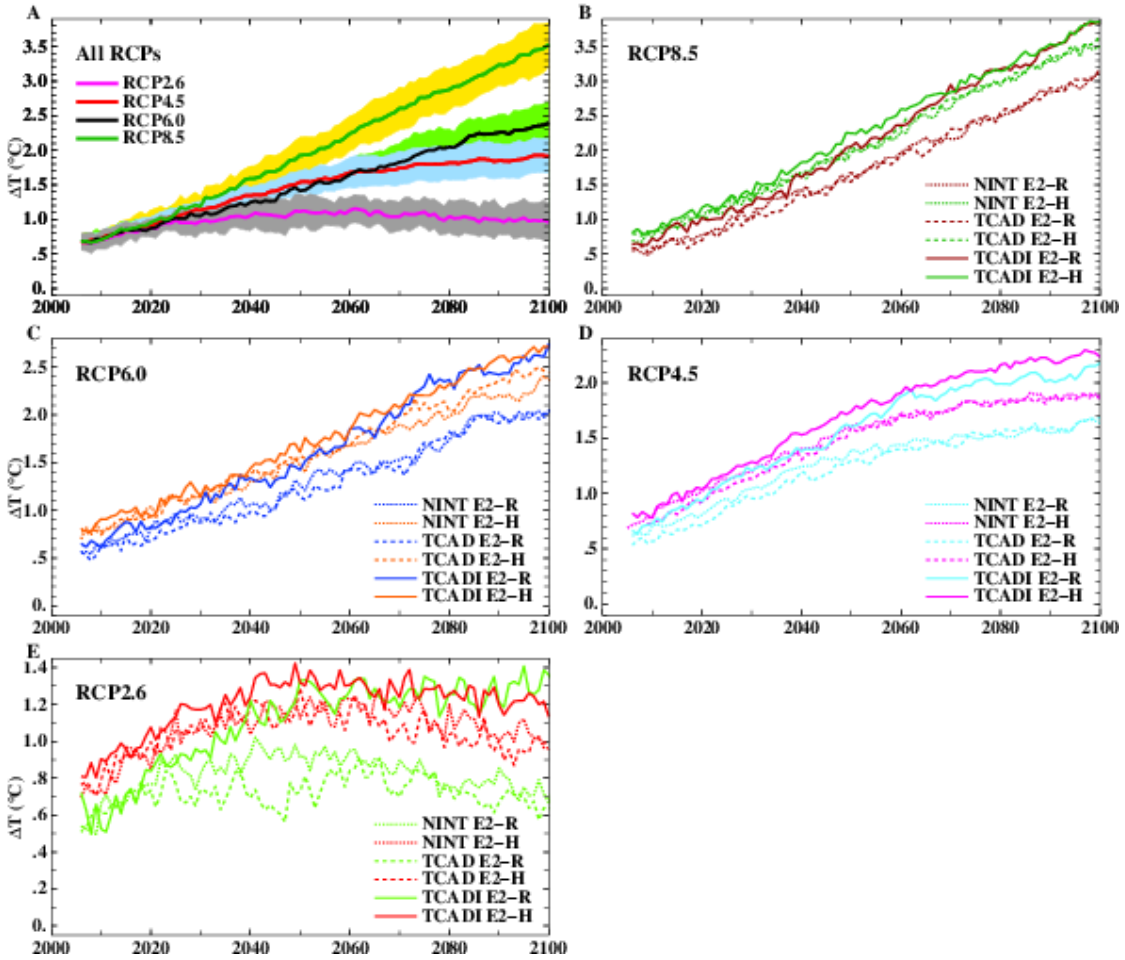

Global surface air temperature anomalies relative to 1951-1980 base period for annual means.

a. RCP2.6 - 0.4°C to 1.1°C warming at 2050; decrease of warming - 0.2°C to 1.0°C at 2100 ;
b. RCP4.5 and RCP6.0 – warming ranges from 1.6°C to 2.7°C;
c. RCP8.5 – strong warming 3.7°C.

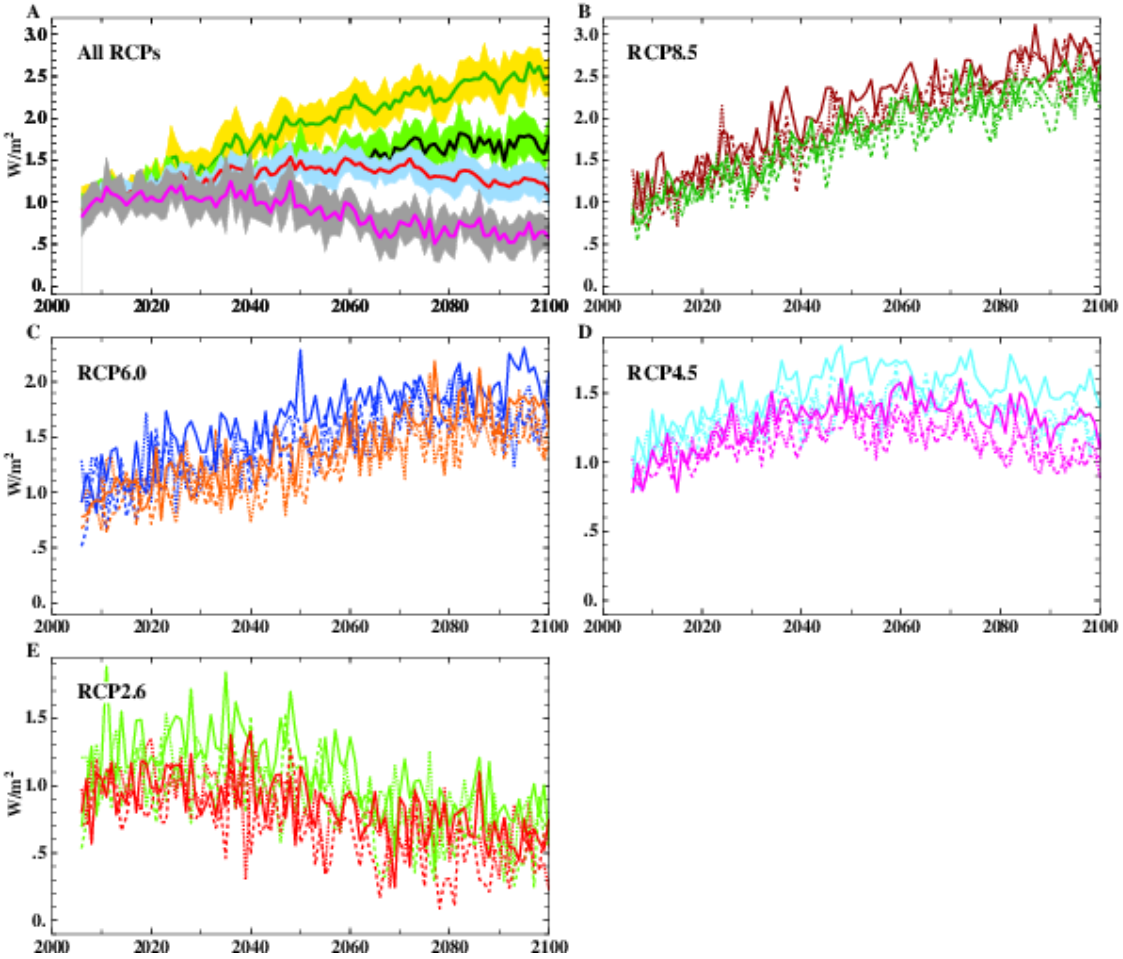

1. RCP2.6 – decline of energy imbalance to half of its max value;
2. RCP4.5 – small decrease of energy imbalance in the last 30-40 years;
3. RCP6.0 and RCP8.5 – continuous increase of energy imbalance.

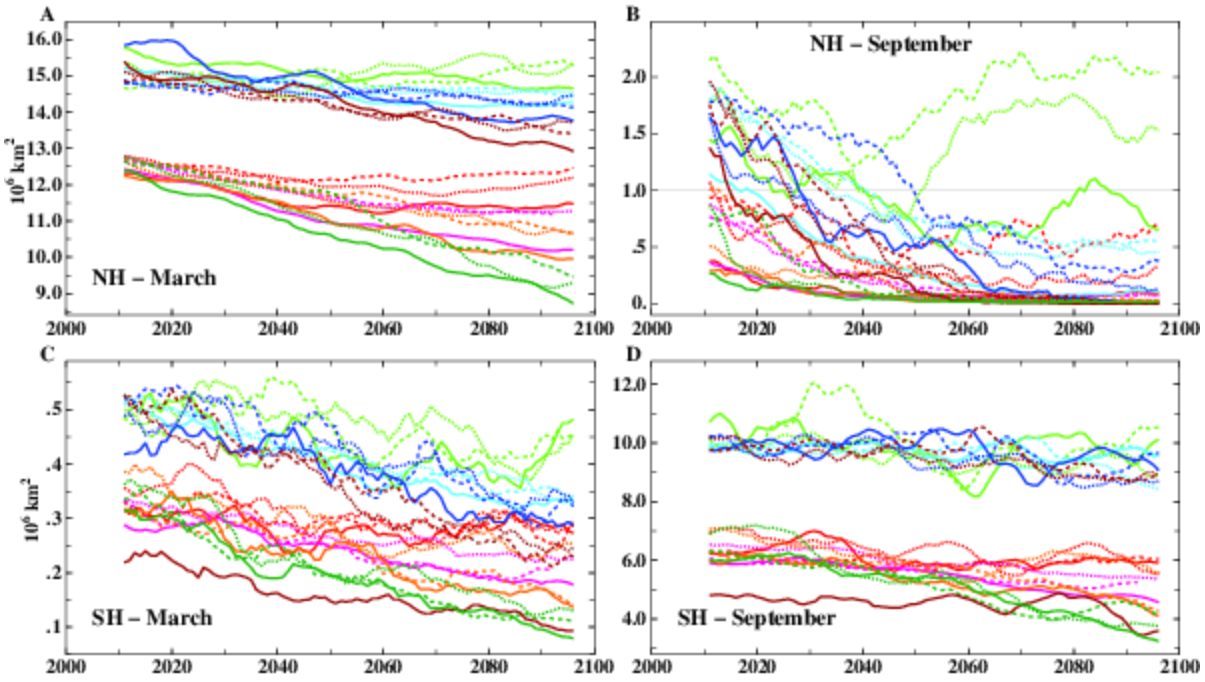

1. Recovery of NH sea ice in RCP2.6 with NINT and TCAD E2-R after 2050; TCADI E2-R – 8% decrease (annual);
2. E2-H shows decrease of annual mean sea ice cover:
   a. RCP2.6 – 11.2% SH (averaged over all three versions NINT, TCAD and TCADI);
   b. RCP4.5 – 16% NH and 12% SH;
   c. RCP6.0 – 19% NH and 16% SH;
   d. RCP8.5 – 32.7% NH and 21.8% SH.
3. E2-H shows decrease of annual mean sea ice cover:
   a. RCP2.6 - 8% NH and 10% SH (averaged over all three versions NINT, TCAD and TCADI);
   b. RCP4.5 – 26% NH and 34% SH;
   c. RCP6.0 – 32% NH and 32% SH;
   d. RCP8.5 - 48% NH and 55% SH.

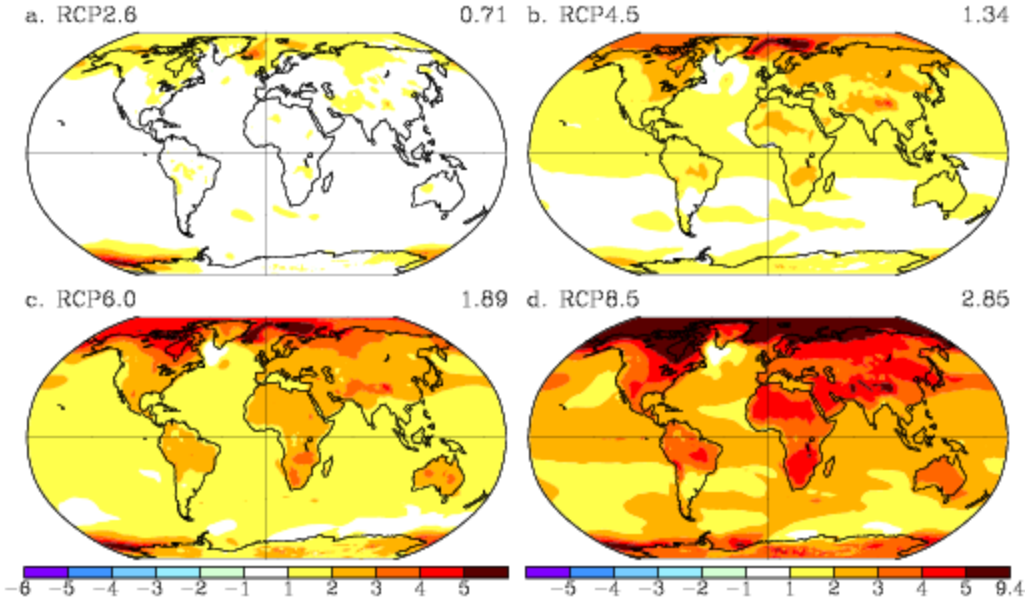

The temperature changes are averaged over the NINT E2-R and E2-H climate models for each RCP scenario for (2081-2100) minus (1986-2005) of the historical simulation.

RCP2.6 warming is 4-5 times smaller than in RCP8.5, and 2-3 times than in RCP4.5 and RCP6.0.

Larger warming over continents than over oceans.

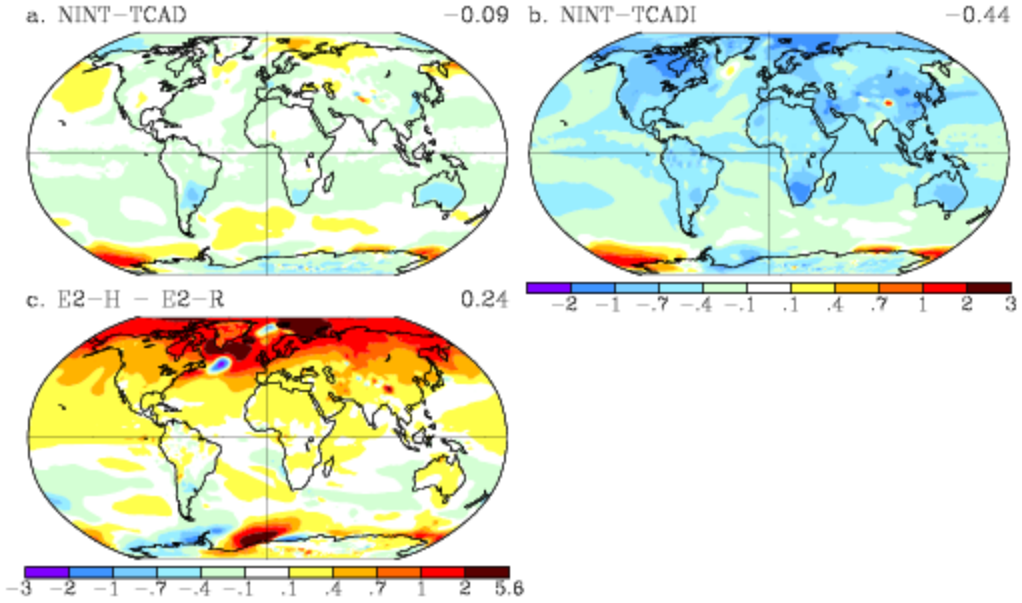

The temperature differences for RCP4.5:

a. TCADI model shows stronger warming due to reduced cloud cover
b. Greater warming over high Northern latitudes in E2-H than in E2-R due to more sea ice melt

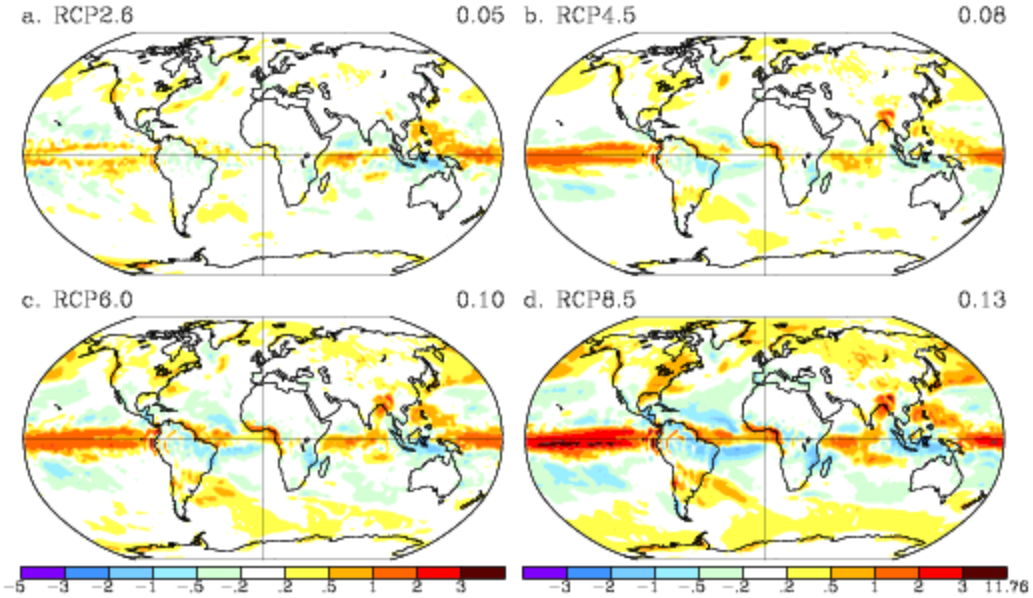

The precipitation changes are averaged over the NINT E2-R and E2-H climate models for each RCP scenario for (2081-2100) minus (1986-2005) of the historical simulation.

Increases in precipitation in the middle and high latitudes due to enhanced poleward transport of moisture from the overall warming and increased atmospheric humidity.

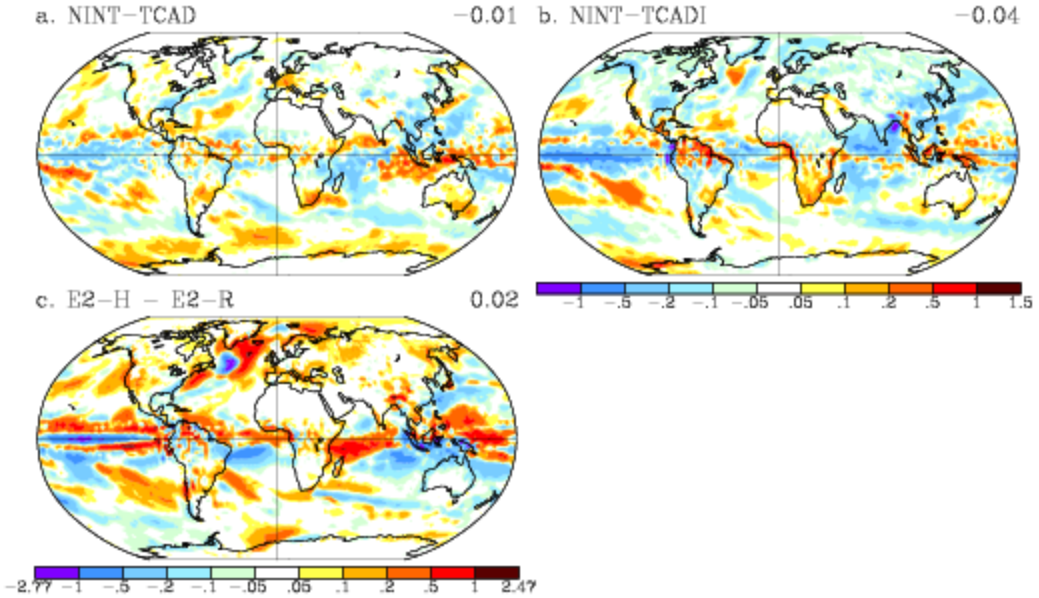

Both the TCAD and TCADI models simulate enhancement of precipitation over the Intertropical Convergence Zone, over the tropical and subtropical ocean areas.

The areas over the Southern Ocean are getting less precipitation with the TCAD and TCADI models due to weaker warming over the these areas compared to the NINT models.

The E2-H climate model produces stronger El Niño-Southern Oscillation (ENSO) variability.

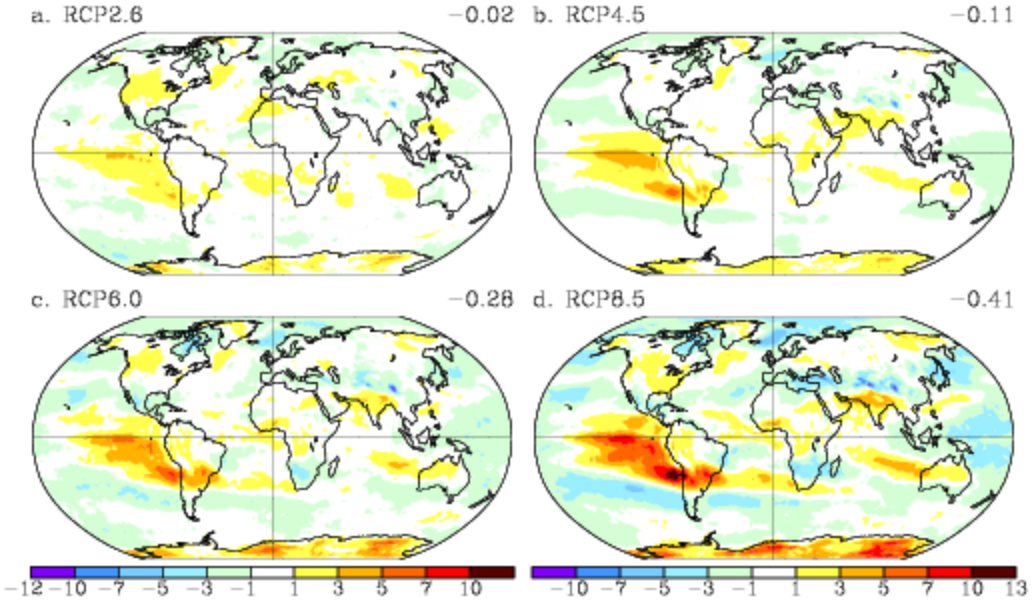

The total cloud cover change:

a. Small overall decrease of cloud cover;
b. Positive feedback or amplification of warming;
c. Increase of clouds over eastern ocean areas;
d. Consistency with changes in precipitation.

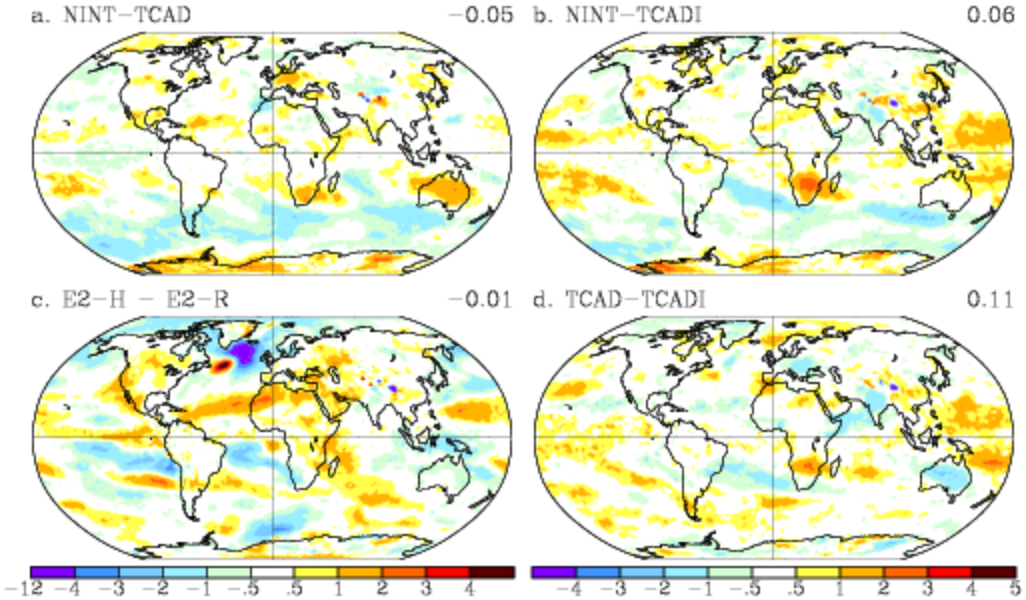

Model differences:

a. NINT fewer clouds + stronger warming over the Southern Ocean;
b. E2-H fewer clouds over the Arctic with contrasting cloud reduction off the east cost of Greenland;
c. TCADI fewer clouds over tropical and sub-tropical ocean areas leads to stronger solar heating and greater warming.

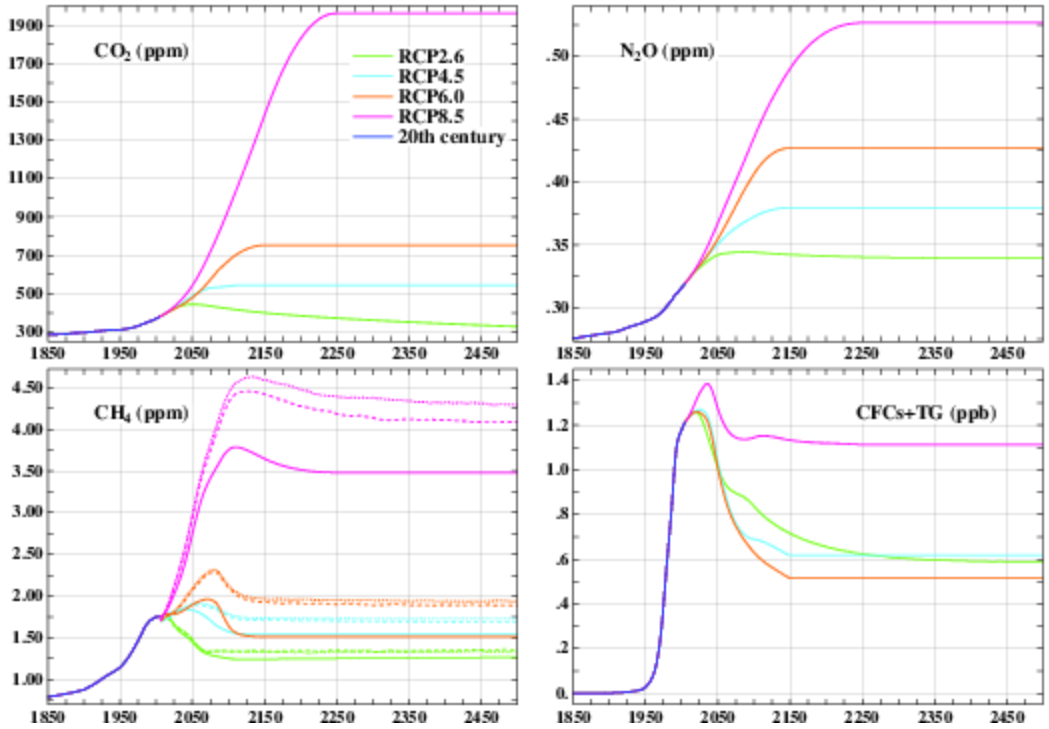

RCP2.6: CO_2 decrease from 421 ppm at 2100 to 328 ppm 2500**;** CFCs and other trace gases from 0.8 ppb at 2100 to 0.6 ppb at 2500; N_2O and CH_4 are kept constant at the year 2100 values.

RCP4.5: CO_2 increase by 4.6 ppm, N_2O – by 0.007ppm from 2100 to 2500; CH_4 decrease by 0.03 ppm, CFC – by 0. 07 ppb by the year 2150.

RCP6.0: CO_2 increase by 82 ppm, N_2O – by 0.02ppm from 2100 to 2500; CH_4 decrease by 0.14 ppm, CFC – by 0. 12 ppb by the year 2150.

RCP8.5: CO_2 increase from 936 ppm at 2100 to 1962 ppm 2500.

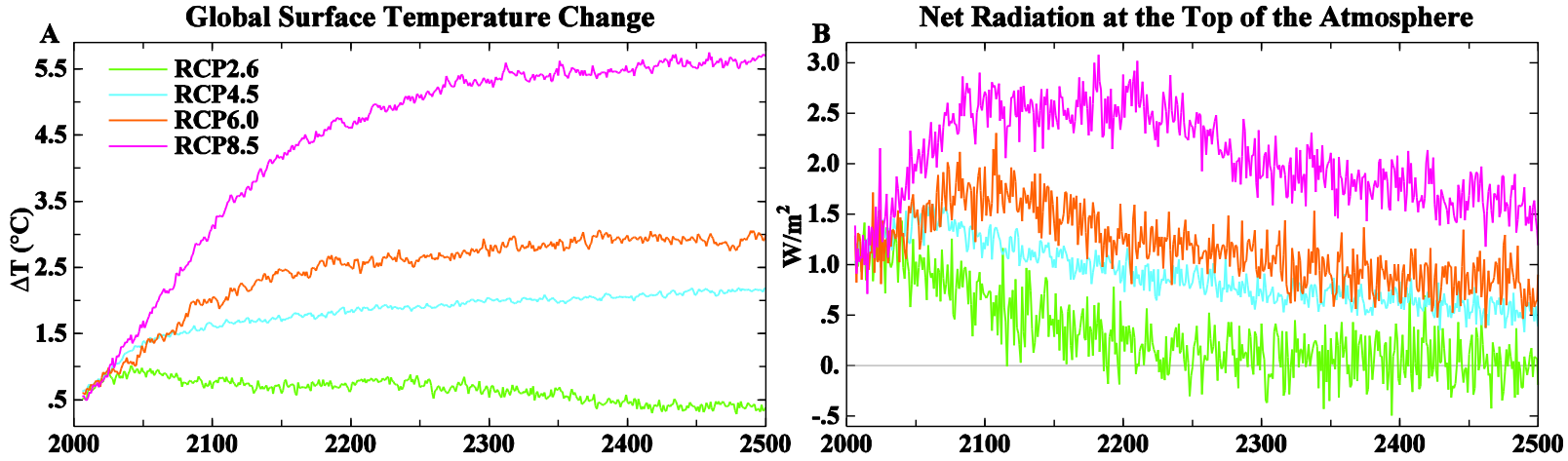

RCP2.6: The recovery of surface air temperature for all versions of the GISS climate model; there is no imbalance by 2300.

RCP4.5: The surface warming ranges between 1.7°C and 2.4°C by 2500; the imbalance is between 0.4 and 0.8 W/m2.

RCP6.0: The surface warming ranges between 2.6°C and 3.5°C by 2500; the imbalance is between 0.5 and 0.9 W/m2.

RCP8.5: The surface warming ranges between 5.3°C and 6.4°C by 2500; the imbalance is between 1.1 and 1.8 W/m2.

Conclusions

- For most years, the GISS-E2 ensemble temperature and the GISTEMP analyzed value are not distinguishable at the level of two standard deviations, even though the GISS-E2-R NINT and TCADI simulations are a little over 0.1K too warm compared to observations by the present-day.
- Warming is larger in the corresponding GISS-E2-H simulations, which is from relatively small heat uptake by the deep ocean compared to the GISS-E2-R ensembles.
- The decrease of the Northern Hemisphere NSIDC sea ice cover is 9.8% from 1979 to 2005 while our model produces a little stronger decline of 10.2% for the Arctic sea ice for the same time period.
- In all RCP scenarios, the calculated methane mixing ratios are larger in both TCAD and TCADI models than in the NINT models. The radiative forcing from methane is from 0.05 to 0.18 W m^2 higher in the TCAD and TCADI models than in the prescribed RCP methane radiative forcing estimates, which leads to larger warming in the TCAD and TCADI models compared to the NINT simulations.
- The high mitigation scenario RCP2.6 is the only one that shows the global warming below 1°C by 2100, which is below the 2°C threshold of dangerous climate change at the end of the twenty-first century relative to the pre-industrial surface temperature.
- For the intermediate RCP4.5 and RCP6.0 and business-as-usual RCP8.5 scenarios, the warming exceeds 1°C by 2100 ranging from 1.1°C in RCP4.5 to 3.7°C in RCP8.5.
- The reduced cloud cover in the fully interactive aerosols and chemistry TCADI climate model leads to stronger warming relative to surface warming in the non-interactive NINT climate model except for a small area over the Southern Ocean.
- In RCP2.6, the weakening of the North Atlantic overturning is 1-3 Sv, which is within the range of the ocean internal variability. In RCP4.5 and RCP6.0, the North Atlantic stream function decreases by 4-10 Sv by 2100 with complete recovery by 2500 in the coupled models with the NINT atmosphere and with partial recovery by 2500 in all other coupled models. Due to the large scale warming, there is a decrease in the overturning stream function by 9-13 Sv in the RCP8.5 experiments in the end of the 21st century. The North Atlantic overturning collapses in the RCP8.5 scenarios around the year 2200 in all coupled models.